Applied Vegetation Science 13: 86–99, 2010
DOI: 10.1111/j.1654-109X.2009.01053.x

Mapping tree species in temperate deciduous woodland using time-series multi-spectral data

R.A. Hill, A.K. Wilson, M. George & S.A. Hinsley

Abstract

Questions: What is the optimum combination of image dates across a growing season for tree species differentiation in multi-spectral data and how does species composition affect overstorey canopy density?

Location: Monks Wood, Cambridgeshire, eastern England, UK.

Methods: Six overstorey tree species were mapped using five Airborne Thematic Mapper images acquired across the 2003 growing season (17 March, 30 May, 16 July, 23 September, 27 October). After image pre-processing, supervised maximum likelihood classification was performed on the images and on all two-, three-, four- and five-date combinations. Relationships between tree species composition and canopy density were assessed using regression analyses.

Results: The image with the greatest tree species discrimination was acquired on 27/10 when the overstorey species were in different stages of leaf tinting and fall. In this image, tree species were mapped with an overall classification accuracy (OCA) of 71% (kappa 0.63). A similar OCA was achieved from the other four images combined (OCA 72%, kappa 0.64). The highest classification accuracy was achieved by combining three images: 17 March, 16 July, 27 October. This achieved an OCA of 84% (kappa 0.79), increasing to 88% (kappa 0.85) after a post-classification clump and sieve procedure. Canopy height and percentage cover of oak explained 72% of variance in canopy density.

Conclusions: The ability to discriminate and map temperate deciduous tree species in airborne multi-spectral imagery is increased using time-series data. An autumn image supplemented with an image from both the green-up and full-leaf phases was optimum. The derived tree species map provides a more powerful ecological tool for determining woodland structural/compositional relationships than field-based measures.

Keywords: Airborne thematic mapper (ATM); Canopy density; Classification; Forest; Image; Phenology; Remote sensing.

Nomenclature: Steele & Welch (1973).

Hill, R.A. (corresponding author, rhill@bournemouth.ac.uk): Bournemouth University, Talbot Campus, Poole, Dorset BH12 5BB, UK.
Wilson, A.K. (akw@ceh.ac.uk) & **Hinsley, S.A.** (sahi@ceh.ac.uk): Centre for Ecology and Hydrology, Monks Wood, Huntingdon, Cambs PE28 2LS, UK.
George, M. (mgeorge@caci.co.uk): CACI Limited, Thomas Yeoman House, The Canal Basin, Coventry CV1 4LW, UK.

Introduction

The ability to map tree species across woodland is important for habitat assessment and effective forest management. Overstorey tree species composition has a significant influence on habitat quality and forest structure. For example, overstorey canopy density and composition has a primary influence on woodland structure and composition at lower levels via shading and the abundance and distribution of gaps (Holmes & Sherry 2001; Lhotka & Loewenstein 2008). In addition, overstorey trees also influence the availability to the understorey of other resources, such as water and nutrients, and can modify the chemical characteristics of the litter layer (Barbier et al. 2008), which in turn can affect understorey diversity (van Oijen et al. 2005).

Remote sensing techniques, especially optical imagery, have long been investigated and employed for forest assessment. However, mapping tree species in optical imagery is a difficult task as spectral variation within species is typically greater than between them (Wolter et al. 1995; Lucas et al. 2008). Factors influencing and increasing within-species spectral variation in a remotely sensed optical image include: illumination and view angle differences, natural variability in canopy structure and openness, shadowing effects, and crown health (Leckie et al. 2005a). As a result, considerable variation has been reported in the accuracy of species mapping in single-date optical imagery. This is true both in terms of variation in the accuracy with which individual species have been mapped at a particular site and variation in overall accuracy of tree species mapping reported between studies at different sites

(Carleer & Wolff 2004; Gougeon & Leckie 2006; Greenberg et al. 2006).

For deciduous woodland, difficulties of tree species classification in spectral data can be at least partly overcome by the use of time-series data (Schriever & Congalton 1995; Mickelson et al. 1998). The reflectance characteristics of a deciduous forest will vary through the leaf phenological cycle resulting from changes in the biophysical or biochemical attributes of the canopy (Miller et al. 1991; Kodani et al. 2002). Seasonal variations in spectral reflectance are pronounced both within deciduous species (Boyer et al. 1988; Blackburn & Milton 1995) and between them (Key et al. 2001). Time-series optical data that capture phenological change, such as leaf flush or senescence, are thus likely to increase the spectral separability of deciduous tree species. This occurs either when they are in different phenological stages in the same image or when they undergo phenological change at different rates between images over a growing season (Dymond et al. 2002).

All of the early papers investigating the application of time-series optical data for forest classification were unable to collect images from across a single growing season. Schriever & Congalton (1995) classified seven different hardwood forest cover types in New Hampshire using satellite-derived Landsat Thematic Mapper (TM) data acquired in May 1988, September 1990 and October 1989. Although acquired from different years, the images represented conditions of bud break, leaf on and senescence, respectively. Wolter et al. (1995) adopted a layered approach to the multi-temporal classification of hardwood forest species in the northern Lake States region of the USA. This made use of a Landsat TM image acquired in June 1987 to achieve an Anderson Level II forest classification. Multi-temporal Landsat Multi Spectral Scanner (MSS) imagery acquired in February 1988, May 1992, September 1985 and October 1980 were subsequently analysed to target specific phenological trends associated with key tree species. Mickelson et al. (1998) combined spectral data from the six reflective bands of multi-temporal Landsat TM data (May 1988, August 1990, and October 1992) to produce a forest type map of the dominant canopy species in mixed deciduous forests of north-western Connecticut, USA. Dymond et al. (2002) examined four Landsat TM images (May 1992, August 1993, September 1992 and October 1991) to map deciduous forest at the genus level in the northern hardwood region of Wisconsin, USA. They employed a method of image differencing Tassled Cap indices, which were reported to emphasize both the structural and phenological differences between vegetation types across image dates.

To date the only study to examine time-series digital data acquired across a single growing season for forest species mapping is that of Key et al. (2001). They investigated the classification of individual tree species using RGB and CIR aerial photographs acquired on nine dates across the 1997 growing season for Eastern Deciduous Forest in West Virginia, USA.

In this paper we investigated the ability to discriminate and map overstorey tree species based on their spectral signatures (in the visible to short wave infrared spectrum) over time across a single growing season. The study area was an ancient, semi-natural wood composed of broadleaf deciduous species. We examined five dates of airborne multi-spectral imagery, which capture information across a growing season from green-up to senescence. The aim was to investigate how the spectral separability of six deciduous tree species changes (1) in individual images acquired across a growing season and (2) when images acquired on different dates are examined in different combinations. The objectives were threefold. First, to assess the optimum timing of data acquisition and the optimum combination of image dates to increase tree species differentiation. Second, to produce an overstorey tree species map as an additional geo-spatial input to on-going bird habitat assessment work at the study site (Hill et al. 2004; Broughton et al. 2006; Hinsley et al 2002, 2006, 2008). Third, to investigate how tree species composition influences canopy density. In previous work we demonstrated the ability of canopy height to predict overstorey canopy density (Hinsley et al. 2002), and here we examined the effects of tree species composition on this relationship. In addition to the influence of overstorey canopy on subcanopy woodland structure and resources mentioned above, canopy density is fundamental for woodland bird community composition and distribution (Hinsley et al. 2009) and, in conjunction with tree species identity, a major determinant of foraging habitat quality (Hinsley et al. 2008).

Materials and Methods

Field site

The study area was Monks Wood National Nature Reserve in Cambridgeshire, eastern England (52°24′N, 0°14′W). This is an ancient wood of broadleaf deciduous species, which covers 157 ha. The geology of the study area is dominated by grey

calcareous Oxford clay, chalky boulder clay and calcareous clay with loamy and sandy drift (Steele & Welch 1973). These deposits give rise to base-rich soils: gleyic brown calcareous earths and surface water gleys. The canopy species composition of Monks Wood is dominated by the influence of the drainage conditions, base-rich soils and management history.

Monks Wood is extremely heterogeneous in terms of the woody species making up the tree canopy and understorey, their relative proportions in any area, and canopy closure and density (Patenaude et al. 2004; Hill & Thomson 2005). The overstorey tree species of Monks Wood are common ash (*Fraxinus excelsior*), English oak (*Quercus robur*), field maple (*Acer campestre*), silver birch (*Betula pendula*), aspen (*Populus tremula*) and small-leaved elm (*Ulmus carpinifolia*). Common ash is the most common and widespread species, occurring mostly as coppice stems but regenerating naturally wherever the canopy is opened (Massey & Welch 1993). English oak occurs less frequently because of intense felling during the early Twentieth Century. Field maple and silver birch are found scattered throughout Monks Wood, while aspen and small-leaved elm form occasional clusters on the wetter soils. Small-leaved elm declined significantly in the 1970s because of an outbreak of Dutch elm disease (*Ophiostoma novo-ulmi*). The former elm stands were left to regenerate naturally and tend to be rather scrubby in nature. The understorey is variable in nature and scattered throughout Monks Wood (Hill & Broughton 2009). The dominant woody species making up the understorey and fringes of Monks Wood are hawthorn (*Crataegus monogyna*), common hazel (*Corylus avellana*), blackthorn (*Prunus spinosa*), dogwood (*Cornus sanguinea*) and common privet (*Ligustrum vulgare*). Hazel, along with ash, was coppiced until 1995. Hazel now occurs mixed with hawthorn and blackthorn throughout Monks Wood (Massey & Welch 1993). Also to be found in the more open areas, are elder (*Sambucus nigra*), buckthorn (*Rhamnus catharticus*), grey willow (*Salix cinerea*), goat willow (*Salix caprea*), downy birch (*Betula pubescens*), crab apple (*Malus sylvestris*) and bramble (*Rubus fruticosus*).

Field data collection

A survey was carried out across Monks Wood in July 2005 to identify the location of a sample of trees for each overstorey species. A series of temporary benchmarks was established systematically along paths and rides in Monks Wood by real-time kinematic (RTK) survey with a differential Global Positioning System (GPS). The base station was set up initially on a calibration target immediately south of the woods, for which the coordinates were known to better than 10 mm accuracy in x, y and z. On subsequent survey days (six in total) the base station was set up at an intersection of rides within Monks Wood where a wider horizon was exposed. From each benchmark the location of individual trees of identified species was recorded as a distance and bearing using a tape measure and compass. This totalled 299 individual trees identified by species across the field site. Sample size per species varied from 20 trees for small-leaved elm, 36 trees for both aspen and silver birch, 39 trees for field maple, and 84 trees for both common ash and English oak.

Field estimates of tree species composition in the overstorey canopy, and of canopy density were made independently by two observers (and results expressed as mean values) in the summer of 2001. The percentage of overstorey canopy cover within a 54 m × 54 m sample area attributable to each tree species was assessed by eye. Similarly, the proportions of the sample area attributable to each of five density scores (range 0-4, where 0 = absence and 4 = dense, closed canopy) were assessed and an overall canopy density index (CDI) calculated as Σ(score × proportion) (Hinsley et al. 1995). The sample areas were centred on 22 nestboxes located across the study site, the coordinates of which were mapped using a total station (Hinsley et al. 2002).

Image data acquisition and pre-processing

The remotely sensed imagery examined in this study were acquired with a Daedalus 1268 Airborne Thematic Mapper (ATM). This enhanced version of the sensor records a swath width of 938 pixels over a 90° field of view at a scan rate of 50 Hz. The ATM data have 11 bands of fixed wavelength position in the visible, near, short-wave and thermal infrared parts of the electromagnetic spectrum (Table 1). The radiometric resolution of the data is 16-bit. The ATM data were acquired on five dates in 2003: 17 March, 30 May, 16 July, 23 September and 27 October. These dates captured the time-period of green-up and senescence for all six overstorey species.

Monks Wood was covered by two overlapping flight-lines of ATM data on each acquisition date. These were processed to create a single image scene per date, with a spatial resolution of 2 m and

Table 1. The 11 bands of fixed wavelength position recorded by the Daedalus Airborne Thematic Mapper (ATM) sensor used in this study.

Spectral Band	Wavelength (mm)	Spectral region
1	0.42–0.45	Ultraviolet/blue
2	0.45–0.52	Blue
3	0.52–0.60	Green
4	0.60–0.62	Yellow/orange
5	0.63–0.69	Red
6	0.69–0.75	Near-infrared
7	0.76–0.90	Near-infrared
8	0.91–1.05	Near-infrared
9	1.55–1.75	Short-wave infrared
10	2.08–2.35	Short-wave infrared
11	8.50–13.00	Thermal infrared

spectral values calibrated to at-sensor radiance ($\mu W\,cm^{-2}\,sr^{-1}\,nm^{-1}$). To achieve this, individual flight-lines per date were radiometrically calibrated, normalized for limb brightening, geometrically corrected, radiometrically matched and mosaicked using a "wedge" algorithm that preferentially selected pixels closest to nadir in areas of overlap. These stages are described below.

Radiometric calibration of ATM sensor data

The spectral values recorded by the ATM sensor were radiometrically calibrated to at-sensor radiance ($\mu W\,cm^{-2}\,sr^{-1}\,nm^{-1}$). This was achieved by the application of a gain and offset for each of the 10 solar reflective bands, derived from a laboratory-based bench calibration against a source traceable to a national standard (via the National Physics Laboratory). Calibrated data were then multiplied by 1000 to allow subsequent data handling as a 2-byte (16-bit) short integer, without loss of numerical precision.

Across-scan radiometric normalization

Although the images were all radiometrically calibrated to absolute radiance units, visual examination of the individual flight-lines highlighted a limb brightening effect. This was caused by both path length effects and the differential scattering angles of atmospheric aerosols. The ATM data were acquired near to midday, to maximize solar irradiance and signal strength, with the majority flown in a north-south orientation. In this mode the limb brightening resulting from aerosol optical depth was minimized and was symmetrical about the nadir line of the flight-line. For those flown perpendicular to the solar azimuth, limb brightening was greater and asymmetric as a result of the larger variation in scattering angle between the solar zenith/azimuth angle and the across-scan sensor view angle (± 45°).

Radiometric corrections were applied to minimize the limb brightening effect and "flatten" the general upward trend in spectral response towards the edge of each scan line. The data from each acquisition date, comprising 938 pixels by "n" scan lines by 11 spectral bands (where "n" was the different number of scan lines in each of the flight-lines) were sub-sectioned down to a common number of scan lines that covered Monks Wood and its immediate surroundings. Column averages were created for each band of each sub-sectioned flight-line and a third order polynomial curve fitted to these average data. This captured the overall limb brightening for each flight-line. These third-order polynomial curves were then used to normalize each band of each individual flight-line to their nadir values. This minimized the limb brightening effect while retaining local scene variability.

Geometric correction

An Azimuth Systems program (AZGCORR, http://arsf.nerc.ac.uk/data/azimuth.asp) was used to (1) apply the aircraft navigation data to each scan line of the normalized image files and (2) project those data onto a geoid-based projection to determine the exact intersection of each pixel's view angle with a high spatial resolution digital surface model (DSM). The DSM used here had a 1 m spatial resolution and was generated from airborne laser scanning (Gaveau & Hill 2003). This produced a geo-corrected product aligned to the British National Grid, using transformation coefficients and algorithms provided by the Ordnance Survey of Great Britain. The ATM sensor data were resampled to 2 m pixel spatial resolution using a bicubic spline interpolation algorithm.

Each geo-corrected flight-line for each date, was validated for geometric accuracy by overlaying vectors of building outlines, boundary details, road edges, and water features from the Ordnance Survey Land-Line Plus data set. In addition, CEH land bordering Monks Wood contains a set of six geometric targets that have been precisely located to better than 10 mm accuracy. All images were geolocated to better than half a pixel accuracy with reference to these targets and data sets.

Between flight-line radiometric normalization

For each date of image acquisition, a pair of adjacent and overlapping flight-lines was required to provide complete coverage of Monks Wood. In each

case it was noted that there were residual differences in the spectral radiance of target areas within the overlap region. This would have resulted from changes in total illumination between flight-lines and directional view angle effects; in addition, there may have been residual errors in the limb brightening correction procedure. It was therefore necessary to apply a further radiometric correction procedure between flight-lines acquired on the same date, matching median spectral values for identical target patches within the overlap region. This reduced spectral differences between flight-lines acquired on the same date to an insignificant level.

Note that scene matching between the five acquisition dates was not attempted because of the lack of appropriate non-vegetative targets within the study area that would have a stable surface reflectance throughout the entire period.

Image mosaicking based on closeness to nadir

Both the radiometric and geometric accuracy of airborne remotely sensed data are better towards the central nadir viewpoint of an individual flight-line. A method was therefore devised that gave preference to pixels that were closer to the nadir of their respective flight-line during the process of mosaicking overlapping flight-lines for each image acquisition date. Thus in the output mosaicked image, the spectral values at each pixel were taken from whichever of the two overlapping flight-lines recorded that point closest to nadir. This minimized any residual radiometric or geometric errors caused by view angle.

Tree species mapping and analysis

The field data on tree species location were separated randomly within each species into 165 trees for training purposes and 134 trees for validation. For each point identified in the field, a circular plot of 2 m radius was overlaid over each mosaicked ATM image and the spectral information was extracted from the 4 or 5 pixels that constituted the majority of the area covered by each circular plot. This resulted in a training data set totalling 755 pixels and a validation data set of 600 pixels per image date. Individual tree crown delineation was not attempted because of the 2 m image spatial resolution. For the 165 training areas the spectral separability of the six overstorey tree species was examined using Transformed Divergence Analysis and spectral sub-classes were identified per species, where necessary. These were used for supervised maximum likelihood classification. This was carried out per-pixel on the five individual images, and on all two-date, three-date and four-date image combinations and on the five-date combination. Thus, 31 image classifications were carried out in total, each using the same set of 165 training areas, but with a different combination of image dates. Only six wavebands of data per image were used (Bands 3, 5, 6, 7, 8 and 9) to remove data with low signal-to-noise ratio (Bands 1, 2 and 4) and detector problems (Bands 10 and 11). Because of the greater variety of sub-dominant and understorey tree species present across Monks Wood, which would have complicated the classification training process, these were masked out of the ATM images. This was achieved by applying a height threshold of 8 m by overlaying each ATM image with a LiDAR-derived digital canopy height model (Gaveau & Hill 2003). Overstorey trees were therefore considered to have a canopy height of greater than 8 m. This threshold was based on field observation of height for sub-dominant and understorey trees across Monks Wood.

The accuracy of all 31 classification outputs was assessed using the pixel information from the 134 validation areas. Correspondence matrices, including producer's and user's accuracies, overall classification accuracy (OCA) and kappa statistics were calculated for all classification outputs. For the classification output with the highest OCA and kappa statistics, a clump and sieve algorithm was performed in which any group of less than 4 pixels was replaced with the majority class from a 4×4 pixel kernel. The accuracy of this post-processed classification output was also assessed. It is this product that is considered as the final tree species map for the study site.

The proportional cover of each species in the final tree species map was calculated for a sample area of 54 m×54 m (2916 m^2) centred on each of the 22 nestboxes. The proportional cover of each species was calculated as the percentage contribution to the overstorey tree canopy within the sample area. Therefore, for each sample area the total proportional cover of all six tree species equalled 100%. These tree species data supplemented data on mean canopy height extracted as part of previous work (Hinsley et al. 2002) for the same sample areas from a LiDAR-derived digital canopy height model. Relationships between field-based and remote-sensed estimates of tree species canopy cover and between canopy density (CDI), canopy height (CHt) and canopy cover were examined using regression analysis (performed in Minitab version 15, Minitab Ltd, Coventry, UK).

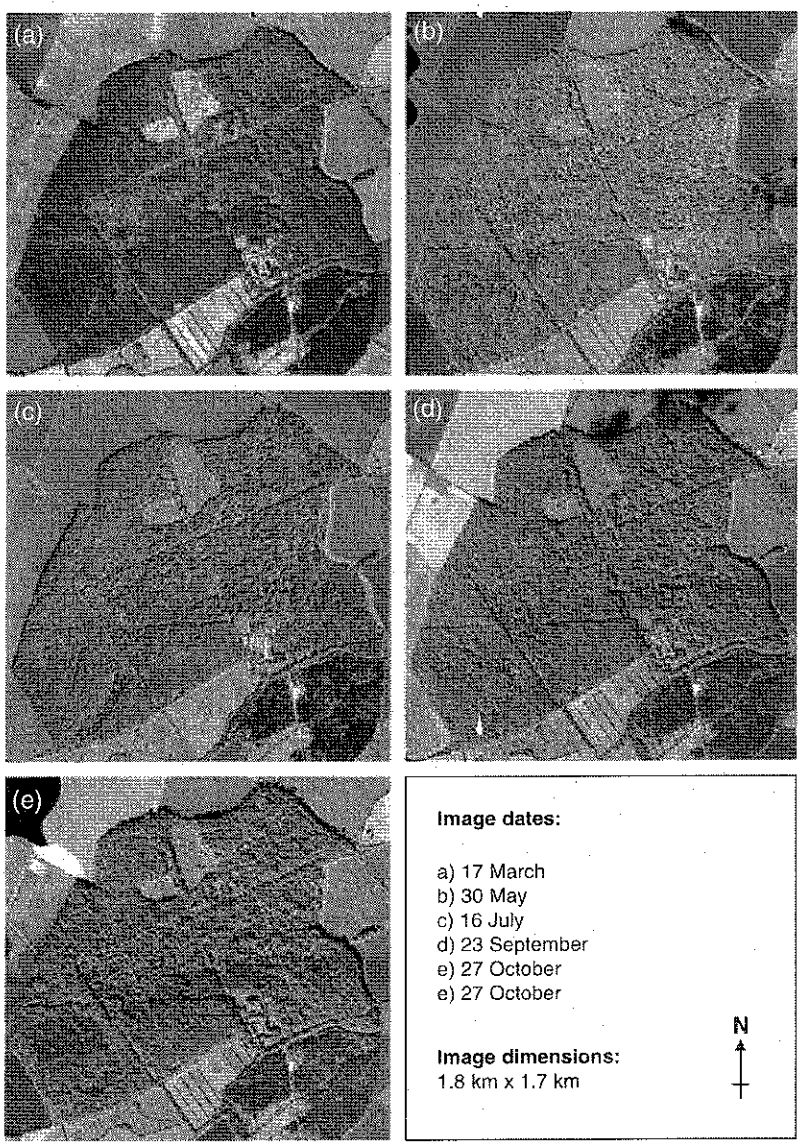

Fig. 1. False colour composite images of the Monks Wood field site (R.G.B. = Airborne Thematic Mapper, ATM, Bands 6, 9, 5) acquired in 2003 on 17 March, 30 May, 16 July, 23 September and 27 October.

Results

Image analysis

The five pre-processed and mosaicked ATM images are shown as false colour composites (RGB: Bands 6, 9, 5) in Fig. 1. From the spectral reflectance curves for the six overstorey tree species on each image date (Fig. 2) it is clear that the greatest difference in the average reflectance characteristics was recorded on 27 October. The average spectral reflectance curves show a degree of separability (but not necessarily between all six species) on 23 September and 17 March, while on 30 May only small-leaved elm has a distinct spectral reflectance curve from the other species and on 16 July all six species have very similar curves.

The overall accuracy of single-date classifications for the six overstorey tree species ranged from 35% (kappa 0.21) on 16 July to 71% (kappa 0.63) on 27 October (Table 2, Fig. 3). The ATM image acquired on 27 October by itself resulted in a higher OCA than all 2-date or 3-date combinations that excluded this image. Furthermore, the four-date

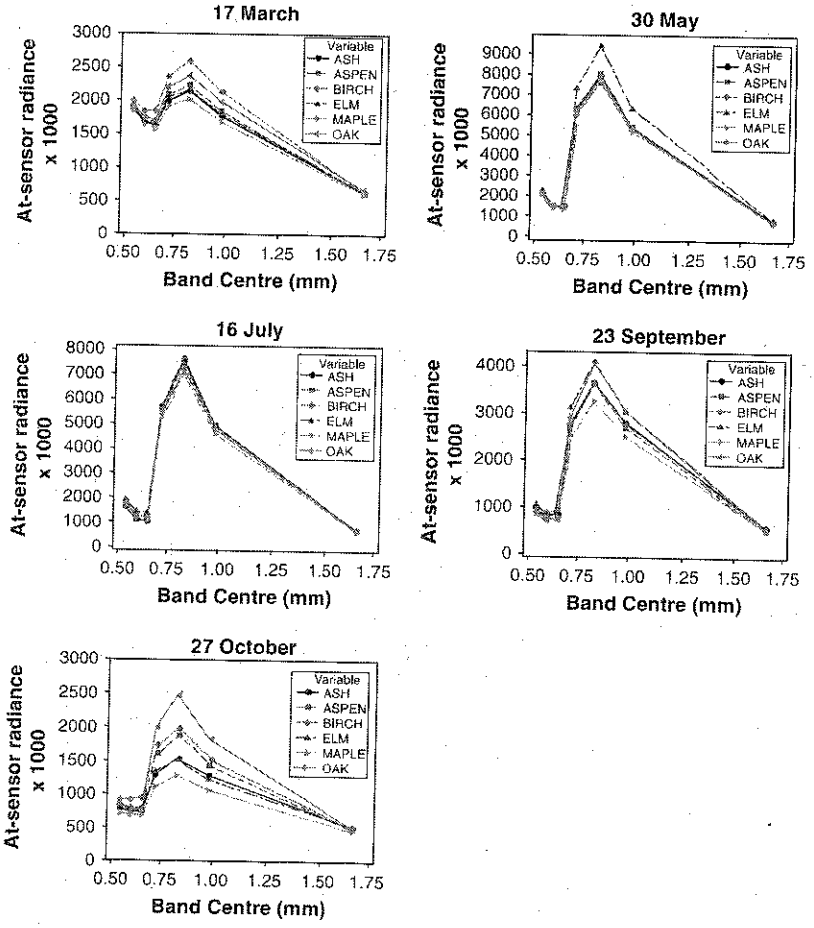

Fig. 2. Spectral reflectance curves (from Airborne Thematic Mapper, ATM, Bands 3-9) for the six overstorey tree species of Monks Wood acquired on five dates in 2003. Values of at-sensor radiance ($\mu W\,cm^{-2}\,sr^{-1}\,nm^{-1}$) have been multiplied by 1000.

combination excluding the 27 October image resulted in a classification with an OCA that was only slightly higher (72%, kappa 0.64) than that of the 27 October image alone.

The two-date combination with the highest OCA (79%, kappa 0.73) involved ATM images acquired on 17 March and 27 October, while the three-date combination with the highest OCA (84%, kappa 0.79) involved images acquired on 17 March, 16 July and 27 October. All four-date combinations and the five-date image combination had an OCA lower than that of the best three-date combination (Table 2, Fig. 3).

The OCA of the best three-date ATM image combination was increased to 88% (kappa 0.85) after a post-classification clump and sieve procedure. In the correspondence matrix for this output (Table 3), statistics for each species are weighted evenly (with 100 validation pixels per species). Producer's accuracies of over 85% were achieved for all tree species except field maple (71%), which was misclassified most frequently as common ash. User's accuracies were over 85% for all tree species except common ash (74%), which was due, in particular, to the errors of commission with field maple. The resultant tree species map can be seen in Fig. 4.

Ecological analysis

For the three most widespread tree species in Monks Wood (common ash, English oak, field maple, Fig. 4), there were significant positive relationships between the field estimates (fe) of percentage canopy cover and the values obtained from the remote sensed (rs) tree species map ($\%ash_{fe} = 25.6 + 0.699\%\ ash_{rs}$, $r^2 = 0.43$, $P = 0.007$, $n = 22$; $\%oak_{fe} = 6.24 + 0.834\ \%\ oak_{rs}$, $r^2 = 0.69$, $P < 0.001$; $\%maple_{fe} = -0.25 + 0.625\ \%\ maple_{rs}$,

Table 2. Overall classification accuracy (OCA) and kappa statistics for the results of mapping six overstorey tree species in a time-series of five Airborne Thematic Mapper (ATM) images. The results for individual image dates are given and for all two-date, three-date, four-date and five-date image combinations.

Image date (day/month)	OCA (%)	kappa
17/03	41.8	0.28
30/05	39.8	0.23
16/07	35.4	0.21
23/09	52.7	0.40
27/10	70.6	0.63
17/03, 30/05	54.2	0.39
17/03, 16/07	51.1	0.38
17/03, 23/09	59.1	0.48
17/03, 27/10	79.0	0.73
30/05, 16/07	48.6	0.35
30/05, 23/09	57.1	0.40
30/05, 27/10	75.4	0.69
16/07, 23/09	59.1	0.40
16/07, 27/10	66.8	0.57
23/09, 27/10	77.5	0.71
17/03, 30/05, 16/07	60.3	0.49
17/03, 30/05, 23/09	69.3	0.60
17/03, 30/05, 27/10	82.3	0.77
17/03, 16/07, 23/09	67.3	0.58
17/03, 16/07, 27/10	83.8	0.79
17/03, 23/09, 27/10	79.0	0.73
30/05, 16/07, 23/09	65.4	0.56
30/05, 16/07, 27/10	79.5	0.74
30/05, 23/09, 27/10	79.2	0.73
16/07, 23/09, 27/10	78.8	0.73
17/03, 30/05, 16/07, 23/09	71.5	0.64
17/03, 30/05, 16/07, 27/10	82.2	0.77
17/03, 30/05, 23/09, 27/10	80.2	0.74
17/03, 16/07, 23/09, 27/10	81.7	0.76
30/05, 16/07, 23/09, 27/10	79.0	0.73
17/03, 30/05, 16/07, 23/09, 27/10	82.2	0.77

$r^2 = 0.46$, $P = 0.001$). The occurrence of the other three species (small-leaved elm, silver birch and aspen) in the sample areas was too uncommon for meaningful comparison. Thus, the closest agreement between field and remote-sensed estimates occurred for English oak (Fig. 5).

There was no significant relationship between canopy density (CDI) and the percentage composition of canopy cover for any of the tree species. This was in contrast to the significant positive relationship ($r^2 = 0.58$, $P < 0.001$, $n = 22$) between CDI and mean canopy height (CHt) established in our previous work (Hinsley et al. 2002). However, including canopy cover of English oak in a multiple regression with canopy height increased the explained percentage variance in CDI ($r^2 = 0.72$, $P_{total} < 0.001$, $n = 22$), but by far the largest effect was from canopy height (Table 4). Including common ash, the most widespread species in the wood, instead of oak made little difference to the r^2 value ($r^2 = 0.61$, $P_{total} < 0.001$, $n = 22$) and $\%ash_{rs}$ was not significant ($P_{ash} = 0.706$). Field maple, gave a similar result to oak ($r^2 = 0.71$, $P_{total} < 0.001$, $n = 22$), but with a negative relationship (Table 4). This was because of a negative relationship between the canopy covers of English oak and field maple ($r^2 = 0.26$, $P = 0.016$, $n = 22$).

Discussion

It is not straightforward to place the results of this study in the context of other published studies that have focused on forest mapping with digital remotely sensed imagery. This is because the nature of the forests examined (especially species composition and structure), forest typology adopted (e.g. genus-level, species-level, physiognomic classes), imagery used (e.g. multi-spectral, hyper-spectral, airborne, space-borne, optical, LiDAR) and methods applied (per-pixel, individual tree crown, single-date, multi-date) differs widely across published studies. Nevertheless, among those studies that have focused on the application of time-series optical data for forest classification, the mapping of six tree species at 88% overall accuracy compares favourably. Thus, Schriever & Congalton (1995) classified seven different hardwood forest cover types in Landsat TM data with an OCA that increased from September (62%) to May (69%) and was highest in October (74%). Mickelson et al. (1998), also using time-series Landsat TM data, achieved a classification accuracy of 79% at the genus level, identifying 33 forest type classes, while Dymond et al. (2002) demonstrated an OCA of 69% (kappa 0.43) for 18 land-cover classes by image differencing Tassled Cap indices. Wolter et al. (1995) distinguished 13 of 22 forest types (with dominant tree species-level precision) with an OCA of 80% using time series Landsat MSS imagery. Lastly, Key et al. (2001) were able to map four deciduous tree species with an overall accuracy of 76% (kappa 0.51) using four available spectral bands but only five of a potential nine aerial photographs.

It should be borne in mind that only dominant trees in the overstorey were mapped in this study. All subdominant and understorey trees were filtered out of the classified products by the application of an 8 m height threshold, via a LiDAR-derived canopy height model. Thus, the full range of woody species present at the study site was not considered. This lowered the possibility for a greater level of spectral overlap to occur between all of the species present. The user's accuracy for the final tree species map would likely be lower if LiDAR data were not available to filter out the more species-rich

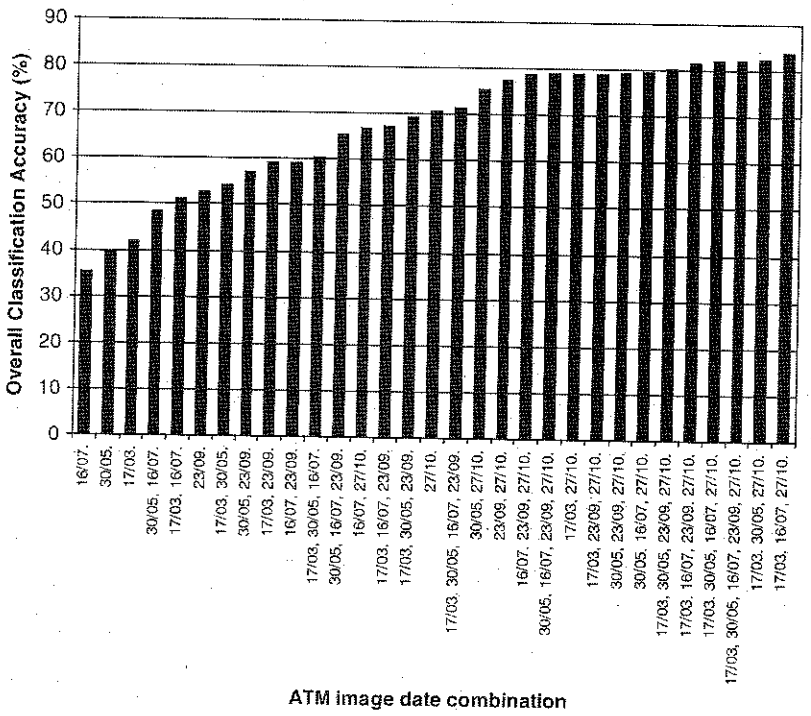

Fig. 3. Plot of overall classification accuracy from the maximum likelihood classification of all single and multi-date Airborne Thematic Mapper (ATM) image combinations.

Table 3. Correspondence matrix for the three-date (17 Mar, 16 Jul, 27 Oct) maximum likelihood classification following a clump and sieve procedure. Individual cell values are pixel counts. The statistics for each species have been weighted evenly and scaled over 100. Abbreviations: UA = user's accuracy, PA = producer's accuracy, OCA = overall classification accuracy.

Class in tree species map	Field reference data						Row total	UA (%)
	Ash	Aspen	Birch	Elm	Maple	Oak		
Ash	94	6	7	4	16	0	126	74
Aspen	3	86	5	4	2	1	99	87
Birch	0	9	89	0	0	2	99	89
Elm	0	0	0	92	6	1	98	94
Maple	4	0	0	0	71	0	75	95
Oak	0	0	0	0	6	97	103	94
Column total	100	100	100	100	100	100	$\Sigma = 600$	
PA (%)	94	86	89	92	71	97		OCA 88

subdominant and understorey trees. The LiDAR data were not incorporated into the classification process itself, as has been successfully demonstrated elsewhere (e.g. Asner et al. 2008; Holmgren et al. 2008), as the focus of this investigation was on multi-spectral data from different dates during the growing season.

The focus of recent studies on forest mapping using remotely sensed data has shifted away from the possibilities of using phenological trends in tree species recognition towards the examination of hyper-spectral and/or hyper-spatial data (Leckie et al. 2005b; Boschetti et al. 2007; Lucas et al. 2008). The results of this study perhaps once more highlight the benefits of time-series data for species classification, although this does require precise geometric and radiometric calibration of imagery. Of obvious benefit to any study contemplating tree species mapping in deciduous woodland is the demonstration that the timing of image acquisition is essential. As reported by previous studies (Schriever & Congalton 1995; Mickelson et al. 1998; Key et al. 2001), the ability to discriminate between forest classes of interest in single-date optical imagery is higher in

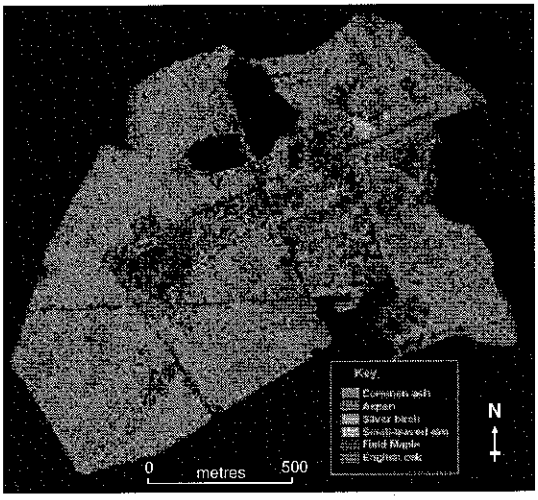

Fig. 4. Tree species map for Monks Wood, produced from the supervised maximum likelihood classification of three Airborne Thematic Mapper (ATM) images acquired in 2003 on 17 March, 16 July and 27 October. The classification output has been subject to a clump and sieve procedure. The map has a pixel size of 2 m and covers an area of 1.8 km × 1.7 km.

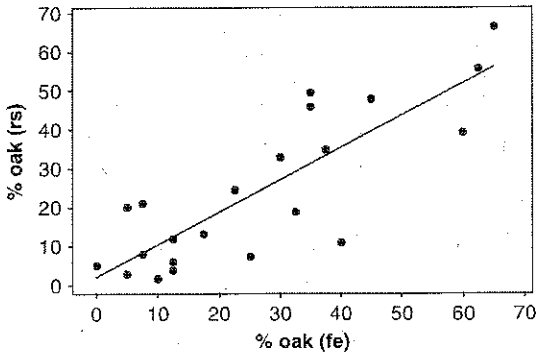

Fig. 5. Relationship between remote sensed (rs) estimates of English oak canopy cover and field-based (fe) estimates of canopy cover for 22 sample areas (2916 m^2) around nest boxes in Monks Wood ($\%oak_{fe} = 6.24 + 0.834\ \%oak_{rs}$, $r^2 = 0.69$, $P < 0.001$).

those data acquired towards the start or end of the growing season than those acquired in mid-summer, with the best timing for image acquisition being mid-autumn. In the study by Schriever & Congalton (1995), they concluded that classification accuracy was highest in late autumn because the factors affecting foliage reflectance characteristics (e.g. leaf biomass, leaf moisture content and chlorophyll content) were at their greatest difference during senescence.

In this study the timing of image acquisition throughout the 2003 growing season was determined largely by logistical constraints (i.e. aircraft availability and suitability of weather conditions). This particularly influenced the acquisition of imagery in the spring. The timing of data acquisition for this study was sub-optimal to capture the processes of budburst and leaf flush in the overstorey. At Monks Wood in 2003, budburst and the onset of leaf flush occurred during April for overstorey tree species. These phenological events therefore took place in the overstorey between the image acquisitions on 17 March and 30 May. The initial stages of greening up apparent in the ATM image acquired on 17 March relate to the understorey, which in 2003 at Monks Wood began budburst predominantly during the first 2 weeks of March. Thus, the apparent onset of greening up for silver birch and English oak in the ATM image acquired on 17 March highlights a greater understorey layer associated with these species, which was exposed in an early state of leaf flush at this time under a leafless overstorey canopy. By 30 May all of the overstorey tree species had leafed out and spectral reflectance curves were similar for all but small-leaved elm. The ideal image acquisition date to capture the different timings of budburst and leaf flush for overstorey tree species in Monks Wood in 2003 would have been late April.

The autumn images were acquired at a time that captured the different stages of leaf tinting and fall during senescence for the different overstorey species. By 23 September the leaves showed a prominent autumn tint on field maple trees and had begun to tint on silver birch, aspen and common ash trees, but not on English oak or small-leaved elm trees. By 27 October field maple, common ash and small-leaved elm trees had reached full leaf tint and were almost half way through leaf fall. Trees of these species were bare by early November. Aspen and silver birch trees had full leaf tint and had begun leaf fall by 27 October, while English oak trees had yet to reach full leaf tint and had not begun leaf fall. Had a final ATM image been acquired in the time-series in mid or late November, this would probably only have distinguished English oak trees.

It is interesting to note that while the two ATM images acquired in the autumn (23 September and 27 October) achieved the most accurate single-date results for tree species mapping, combining these two images did not create the two-date combination with the greatest discriminating ability. This involved the first date (17 March) and last date (27 October) in the time-series. The best three-date

Table 4. Results of regression analyses between canopy density (CDI), canopy height (CHt) and canopy cover by species ($n = 22$ in all cases).

Response variable	Predictor variable	Equation	r^2	P_{CHt}	$P_{tree\ species}$	P_{total}
CDI	CHt	CDI = 0.930+0.080 CHt	$r^2 = 0.58$	< 0.001	–	–
CDI	CHt and %oak	CDI = 0.561+0.097 CHt+0.006 $\%oak_{rs}$	$r^2 = 0.72$	< 0.001	0.012	< 0.001
CDI	CHt and %ash	CDI = 0.931+0.082 CHt – 0.001 $\%ash_{rs}$	$r^2 = 0.61$	< 0.001	0.706	< 0.001
CDI	CHt and %maple	CDI = 0.933+0.090 CHt – 0.006 $\%maple_{rs}$	$r^2 = 0.71$	< 0.001	0.020	< 0.001

combination involved the first (17 March), middle (16 July) and last (27 October) dates in the time-series. Thus combining images that individually did not necessarily offer a strong ability to discriminate between tree species did lead to their successful discrimination owing to differential rates of green-up (predominantly in their associated understorey) and senescence.

The fact that the best single-date image (27 October) resulted in an OCA approximately the same as the four other image dates combined, demonstrated that image quality (in terms of timing) is more significant than image quantity. In addition, the fact that adding extra image dates slightly reduced OCA from the best three-date combination was a demonstration of the Hughes phenomenon (Hughes 1968) and that the size of the training data, which remained constant across all image classifications, was perhaps inadequate as image number increased. The effect of classification accuracy decreasing with increasing number of image dates was also reported by Key et al. (2001) who ascribed it to difficulties in building large training data sets. The addition of extra images which may contain little additional information but can contain noise associated with co-registration errors, variable canopy illumination and differences in observation and illumination angles can weaken the overall strength of signal relating to species differences.

The results identified at Monks Wood for 2003 cannot be treated as indicative of all years as the timing and nature of phenological events can be affected year-on-year by short-term weather conditions and longer-term climatic factors associated with global change dynamics. For example, the summer and autumn of 2003 was a hot and dry period in southern UK compared with long-term mean weather conditions. Data from a meteorological station at Monks Wood demonstrated that during the period 1 April-31 October 2003 each day, on average, had one extra sunshine hour and a 1.5 °C higher maximum temperature compared with the 30-year running mean. In addition, each month during the period April-October 2003 was drier than the 30-year running mean by an average of 10.4 mm. This was likely to have affected the results by influencing (1) the level of leaf tinting during senescence, and (2) the timing of senescence processes. Thus, the autumn of 2003 was particularly colourful as the sustained hot and dry conditions over late summer and autumn would have resulted in the concentration of sugars and anthocyanin in leaves. This enhanced autumnal leaf tinting may have increased the differentiation between species compared with years of more average weather conditions. The timing of leaf tinting was also affected by the hot and dry conditions in 2003, taking place earlier than in more typical weather conditions.

The derived tree species map provided estimates of canopy composition that showed good agreement with the field-base estimates. However, the former provides a more powerful ecological tool that is not limited by access, location or size/shape of sample area. Field-based estimates become difficult for areas larger than about 30 m from a central point and for areas that are irregular in shape. Dense understorey vegetation may also impede ground-based views of the canopy. The validated tree species map has been used as input for understorey modelling, separating within- and below-canopy laser pulse returns in leaf-on and leaf-off LiDAR data (Hill & Broughton 2009) and for the assessment of habitat quality for woodland birds (Hinsley et al. 2008).

Given that leaf and canopy morphology vary greatly between tree species, we expected that tree species contribution to canopy cover would influence the CDI; for example, by eye, the canopies of English oak and field maple appear denser than those of common ash. Our results show that height is the major determinant of canopy density, although for any given height the canopy density increases with the presence of English oak and decreases with the presence of field maple. Thus, in our sample plots, height is providing a surrogate measure for age-related structure and maturity. This concurs with recent results from our work indicating that woodland canopy height can act as an effective surrogate for a suite of characteristics related to woodland structure and development (Hinsley et al. 2002) and can be used as a predictor of woodland

bird community composition and distribution (Hinsley et al. 2009). This is also consistent with previous work in European woodland/forest which has found structure to be more important for bird communities than tree/shrub species composition (Helle & Mönkkönen 1990; Moskát & Fuisz 1994; Fuller & Green 1998).

Conclusions

The ability to discriminate and map temperate deciduous tree species was examined in airborne multi-spectral imagery acquired across a single growing season. The timing of image acquisitions was determined by logistical considerations and was not optimum (in particular, a springtime acquisition in late April would have captured inter-specific differences in the green-up phase). However, results were in agreement with those reported elsewhere, demonstrating that a temporal approach to tree species mapping is robust. From the imagery available, it was shown that quality of imagery, in terms of timing to capture those periods in the leaf phenological cycle when differences between species are greatest, is far more significant than quantity of imagery. Autumn images were shown to have a higher discriminating ability than spring or summer images, but the combination of data from across the entire growing season achieves a greater discrimination than single date imagery alone. Thus, a carefully targeted autumn image acquisition provides a more significant contribution to deciduous woodland species classification, than a large number of additional, sub-optimally timed acquisitions in the rest of the year. Nonetheless, a well-targeted autumn image supplemented with an image from both the green-up and full-leaf phases would appear to be optimum. Additional work is required to be able to predict the optimal timing for image acquisition during greening-up and senescence phases, which will vary from year to year with weather patterns.

The tree species map produced in this study will form an additional data layer in ongoing bird habitat quality assessment work at Monks Wood. Relationships between canopy height, canopy density and tree species composition are fundamental to woodland ecology. This study has shown that species type has relatively little influence on canopy density, with age-related structure (as indicated by height) being the major determinant. Extending the results presented here to other woods, especially of different tree species compositions, will improve our ability to assess habitat quality for a range of taxa and to predict the consequences of potential future changes in woodland (Mason 2007).

Acknowledgements. The data used in this study were acquired by the NERC Airborne Research and Survey Facility (ARSF). This work was carried out while all four authors were based at the Centre for Ecology and Hydrology at Monks Wood, UK.

References

Asner, G.P., Knapp, D.E., Kennedy-Bowdoin, T., Jones, M.O., Martin, R.E., Boardman, J. & Hughes, R.F. 2008. Invasive species detection in Hawaiian rainforests using airborne imagine spectroscopy and LiDAR. *Remote Sensing of Environment* 112: 1942–1955.

Barbier, S., Gosselin, F. & Balandier, P. 2008. Influence of tree species on understory vegetation diversity and mechanisms involved – a critical review for temperate and boreal forests. *Forest Ecology and Management* 254: 1–15.

Blackburn, G.A. & Milton, E.J. 1995. Seasonal variations in the spectral reflectance of deciduous tree canopies. *International Journal of Remote Sensing* 16: 709–720.

Boschetti, M., Boschetti, L., Oliver, S., Casati, L. & Canova, I. 2007. Tree species mapping with airborne hyper-spectral MIVIS data: the Ticino Park study case. *International Journal of Remote Sensing* 28: 1251–1261.

Boyer, M., Miller, J., Belanger, M. & Hare, E. 1988. Senescence and spectral reflectance in leaves of northern pin oak (*Quercus palustris* Muenchh.). *Remote Sensing of Environment* 25: 71–87.

Broughton, R.K., Hinsley, S.A., Bellamy, P.E., Hill, R.A. & Rothery, P. 2006. Marsh Tit territory structure in a British broadleaved woodland. *Ibis* 148: 744–752.

Carleer, A. & Wolff, E. 2004. Exploitation of very high resolution satellite data for tree species identification. *Photogrammetric Engineering & Remote Sensing* 70: 135–140.

Dymond, C.C., Mladenoff, D.J. & Radeloff, V.C. 2002. Phenological differences in Tassled Cap indices improve deciduous forest classification. *Remote Sensing of Environment* 80: 460–472.

Fuller, R.J. & Green, G.H. 1998. Effects of woodland structure on breeding bird populations in stands of coppiced lime (*Tilia cordata*) in western England over a 10-year period. *Forestry* 71: 199–218.

Gaveau, D.L.A. & Hill, R.A. 2003. Quantifying canopy height underestimation by laser pulse penetration in small-footprint airborne laser scanning data. *Canadian Journal of Remote Sensing* 29: 650–657.

Gougeon, F.A. & Leckie, D.G. 2006. The individual tree crown approach applied to Ikonos images of a coniferous plantation area. *Photogrammetric Engineering & Remote Sensing* 72: 1287–1297.

Greenberg, J.A., Dobrowski, S.Z., Ramirez, C.M., Tuil, J.L. & Ustin, S.L. 2006. A bottom-up approach to vegetation mapping of the Lake Tahoe Basin using hyperspatial image analysis. *Photogrammetric Engineering & Remote Sensing* 72: 581–589.

Helle, P. & Mönkkönen, M. 1990. Forest successions and bird communities: theoretical aspects and practical implications. In: Keast, A. (eds.) *Biogeography and ecology of forest bird communities*. pp. 299–318. SPB Academic Publishing, The Hague, NL.

Hill, R.A. & Broughton, R.K. 2009. Mapping understorey from leaf-on and leaf-off airborne LiDAR data of deciduous woodland. *ISPRS Journal of Photogrammetry and Remote Sensing* 64: 223–233.

Hill, R.A. & Thomson, A.G. 2005. Mapping woodland species composition and structure using airborne spectral and LiDAR data. *International Journal of Remote Sensing* 26: 3763–3779.

Hill, R.A., Hinsley, S.A., Gaveau, D.L.A. & Bellamy, P.E. 2004. Predicting habitat quality for Great Tits (*Parus major*) with airborne laser scanning data. *International Journal of Remote Sensing* 25: 4851–4855.

Hinsley, S.A., Bellamy, P.E., Newton, I. & Sparks, T.H. 1995. Habitat and landscape factors influencing the presence of individual breeding bird species in woodland fragments. *Journal of Avian Biology* 26: 94–104.

Hinsley, S.A., Hill, R.A., Gaveau, D.L.A. & Bellamy, P.E. 2002. Quantifying woodland structure and habitat quality for birds using airborne laser scanning. *Functional Ecology* 16: 851–857.

Hinsley, S.A., Hill, R.A., Bellamy, P.E. & Baltzer, H. 2006. The application of LiDAR in woodland bird ecology: climate, canopy structure and habitat quality. *Photogrammetric Engineering and Remote Sensing* 72: 1399–1406.

Hinsley, S.A., Hill, R.A., Bellamy, P.E., Harrison, N.M., Speakman, J.R., Wilson, A.K. & Ferns, P.N. 2008. Effects of structural and functional habitat gaps on woodland birds: working harder for less. *Landscape Ecology* 23: 615–626.

Hinsley, S.A., Hill, R.A., Fuller, R.J., Bellamy, P.E. & Rothery, P. 2009. Bird species distributions across woodland canopy structure gradients. *Community Ecology* 10: 99–110.

Holmes, R.T. & Sherry, T.W. 2001. Thirty-year bird population trends in an unfragmented temperate deciduous forest: importance of habitat change. *Auk* 118: 589–610.

Holmgren, J., Persson, Å. & Söderman, U. 2008. Species identification of individual trees by combining high resolution liDAR data with multi-spectral images. *International Journal of Remote Sensing* 29: 1537–1552.

Hughes, G.F. 1968. On the mean accuracy of statistical pattern. *IEEE Transactions of Information Theory* IT-14: 55–63.

Key, T., Warner, T.A., McGraw, J.B. & Fajvan, M.A. 2001. A comparison of multispectral and multitemporal information in high spatial resolution imagery for classification of individual tree species in a temperate hardwood forest. *Remote Sensing of Environment* 75: 100–112.

Kodani, E., Awaya, Y., Tanaka, K. & Matsumura, N. 2002. Seasonal patterns of canopy structure, biochemistry and spectral reflectance in a broad-leaved deciduous *Fagus crenata* canopy. *Forest Ecology & Management* 167: 233–249.

Leckie, D.G., Tinis, S., Nelson, T., Burnett, C., Gougean, F.A., Cloney, E. & Paradine, D. 2005a. Issues in species classification of trees in old growth conifer stands. *Canadian Journal of Remote Sensing* 31: 175–190.

Leckie, D.G., Gougean, F.A., Tims, S., Nelson, T., Burnett, C.N. & Paradine, D. 2005b. Automated tree recognition in old growth conifer stands with high resolution digital imagery. *Remote Sensing of Environment* 94: 311–326.

Lhotka, J.M. & Loewenstein, E.F. 2008. Influence of canopy structure on the survival and growth of underplanted seedlings. *New Forests* 35: 89–104.

Lucas, R., Bunting, P., Paterson, M. & Chisholm, L. 2008. Classification of Australian forest communities using aerial photography, CASI and HyMap data. *Remote Sensing of Environment* 112: 2088–2103.

Mason, W.L. 2007. Changes in the management of British forests between 1945 and 2000 and possible future trends. *Ibis* 149(Suppl. 2): 41–52.

Massey, M.E. & Welch, R.C. 1993. *Monks Wood National Nature Reserve: The experience of 40 years 1953–1993*. English Nature, Peterborough, UK.

Mickelson, J.G., Civco, D.L. & Silander, J.A. 1998. Delineating forest canopy species in the Northeastern United States using multi-temporal TM imagery. *Photogrammetric Engineering & Remote Sensing* 64: 891–904.

Miller, J.R., Wu, J., Boyer, M.G., Belanger, M. & Hare, E.W. 1991. Seasonal patterns in leaf reflectance red-edge characteristics. *International Journal of Remote Sensing* 12: 1509–1523.

Moskát, C. & Fuisz, T. 1994. Forest management and bird communities in the beech and oak forests of the Hungarian Mountains. In: Hagemeijer, E.J.M. & Verstrael, T.J. (eds.) *Bird numbers 1992. Distribution, monitoring and ecological aspects. Proceedings of the 12th International Conference of IBCC and EOAC, Noordwijkerhout, The Netherlands*. pp. 29–38. Statistics Netherlands, Voorburg/Heerlen & SOVON, Beek-Ubbergen, NL.

Patenaude, G., Hill, R.A., Milne, R., Gaveau, D.L.A., Briggs, B.B.J. & Dawson, T.P. 2004. Quantifying forest above ground carbon content using LiDAR remote sensing. *Remote Sensing of Environment* 93: 368–380.

Schriever, J.R. & Congalton, R.G. 1995. Evaluating seasonal variability as an aid to cover-type mapping

from Landsat Thematic Mapper data in the Northeast. *Photogrammetric Engineering & Remote Sensing* 61: 321–327.

Steele, R.C. & Welch, R.C. 1973. *Monks Wood, a nature reserve record.* The Nature Conservancy, Peterborough, UK.

Van Oijen, D., Feijen, M., Hommel, P., den Ouden, J. & de Waal, R. 2005. Effects of tree species composition on within-forest distribution of understorey species. *Applied Vegetation Science* 8: 155–166.

Wolter, P.T., Mladenoff, D.J., Host, G.E. & Crow, T.R. 1995. Improved classification in the northern Lake States using multi-temporal Landsat imagery. *Photogrammetric Engineering & Remote Sensing* 61: 1129–1143.

Received 15 December 2008;
Accepted 16 July 2009.
Co-ordinating Editor: A. Moody